

## Golden Mean Arithmetic in the Fractal Branching of Diffusion-Limited Aggregates

A. Arneodo, F. Argoul, E. Bacry,<sup>(a)</sup> J. F. Muzy, and M. Tabard  
*Centre de Recherche Paul Pascal, Avenue Schweitzer, 33600 Pessac, France*  
 (Received 6 December 1991)

We use the wavelet transform microscope to explore the intricate fractal geometry of Witten and Sander's diffusion-limited aggregates. We report on the discovery of Fibonacci sequences in the internal hierarchical structure of these clusters. We discuss the relevance of the golden mean arithmetic to the numerically well established statistical self-similarity of these aggregates.

PACS numbers: 68.70.+w, 05.40.+j, 64.60.Cn

Fractal growth patterns are common phenomena to a variety of physical, chemical, and biological systems that are driven far from equilibrium by a diffusion field [1]. In this context, the diffusion-limited aggregation (DLA) model introduced by Witten and Sander [2] in 1981 has played a major role since it has stimulated considerable experimental and numerical effort. In this prototype model, an aggregate is grown by the successive accretion of random walkers to the perimeter sites of the cluster. On-lattice and off-lattice computer investigations [1-3] have shown that complex, apparently randomly branched fractals are produced. But despite the appealing simplicity of the DLA model, analytical progress has been very slow and many important theoretical questions remain unanswered. Actually, after nearly ten years of extensive inquiry, only a little is known about the ramified DLA morphology and the understanding of DLA growth remains a very exciting theoretical challenge.

Most of the activity in this field has been focused on the geometrical properties of growing aggregates [1-3]. In the early numerical studies, on-lattice DLA clusters were found to have different scaling properties in the radial and azimuthal directions, raising the question of self-affinity (rather than self-similarity) for these fractal structures [4]. Further large-scale simulations of off-lattice clusters have shown that the existence of two different scaling exponents is only a crossover effect that vanishes in the asymptotic limit of large mass [5]. The statistical monofractality of the DLA clusters is now well admitted and rather accurately established by the measurement of the generalized fractal dimensions that all coincide to the fractal dimension [6-8]:  $D_q = D_F = 1.60 \pm 0.02, \forall q$ . Recently, the application of the wavelet transform [7] (WT) has revealed that this statistical self-similarity is intimately related to the existence of a screening angle distribution (distribution of angles between branches of successive generations) that is scale invariant when exploring the internal inactive region where growth has stopped [9]. This distribution displays a preferential screening angle  $\theta^* = 36^\circ = \pi/5$ . The presence of a pentagonal symmetry, at a macroscopic level, in diffusion-limited aggregation has already been suggested in previous works [10]. The existence of this symmetry at all scales, however, is likely to be a clue to a structural hierarchical ordering. The aim of the present Letter is

to use the wavelet microscope to further inspect the structural implications of this fivefold symmetry and to show that Fibonacci sequences are hidden in the disordered fractal DLA morphology.

For this work we have grown a total of 23 off-lattice DLA clusters with  $10^6$  particles each. For the generation of these clusters we used an efficient algorithm which combines the simplicity of the off-lattice algorithm designed in Ref. [11] with the rapidity of on-lattice hierarchical algorithms [12]. Simulation of large aggregates is necessary as we will primarily concentrate on the extinct region [13] of DLA clusters that can be considered as asymptotic in the sense that it will no longer be modified by further growth. The investigation of scaling properties requires this inner frozen structure to be large enough to resolve several generations of branching. In Fig. 1(a), we show the inner central region of a  $10^6$  particle off-lattice cluster; about  $8 \times 10^4$  particles (corresponding to inaccessible perimeter sites for the random walkers) are contained in a disk of radius  $R = 480$  particle sizes. In Fig. 1(c) are reported the results of box-counting and fixed-mass fractal dimension measurements [6,7]. The generalized fractal dimensions are found to be equal to the fractal dimension:  $D_q = D_F^{DLA} = 1.60 \pm 0.02, \forall q$ . Note that this numerical value is the same, up to the

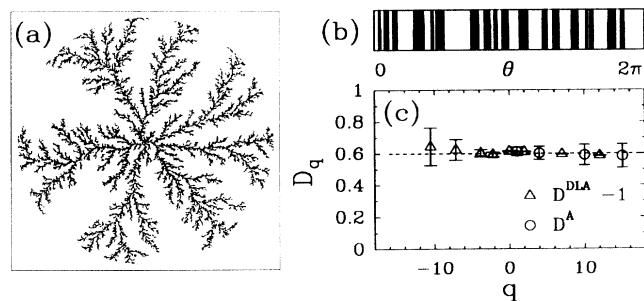


FIG. 1. (a) The inner frozen region of an off-lattice DLA cluster of mass  $M = 10^6$ ; about  $8 \times 10^4$  particles are contained in a disk of radius  $R = 480$  particle sizes. (b) The azimuthal Cantor set defined by the intersection of the DLA cluster with a circle of radius  $R = 480$ . (c) Box-counting ( $q > 0$ ) and fixed-mass ( $q < 0$ ) computation of the generalized fractal dimensions  $D_q$  of the frozen region of the DLA cluster ( $\Delta$ ) and of the azimuthal Cantor set ( $\circ$ ).

computational uncertainty, as for the entire aggregate; this is consistent with the recent numerical demonstration that the subset of inaccessible sites is a fat fractal that involves a finite proportion  $\sim 37\%$  of the total perimeter sites [14]. In Fig. 1(c) are also reported the results of a similar analysis performed on the azimuthal Cantor set defined by the intersection of the DLA cluster with the circle of radius  $R$  that delimits the extinct region. This azimuthal Cantor set [Fig. 1(b)] is also self-similar with a fractal dimension  $D_F^A = 0.60 \pm 0.02$ . The observation that  $D_F^A = D_F^{\text{DLA}} - 1$  is in good agreement with Mandelbrot's argumentation [15] concerning one-dimensional cuts of homogeneous fractals embedded in a two-dimensional space.

As a first step of our demonstration, we will focus our wavelet analysis on the azimuthal Cantor set illustrated in Fig. 1(b). The WT of a measure  $\mu$  with respect to the wavelet  $g$  is defined as [16]

$$T_g[\mu](a,b) = \int \bar{g}\left(\frac{x-b}{a}\right) d\mu(x), \quad a > 0, b \in \mathbb{R}, \quad (1)$$

where the analyzing wavelet  $g$  is generally a regular complex-valued function that is localized around zero and possesses some vanishing moments. A family of commonly used analyzing wavelets is the set of successive derivatives of the Gaussian function. As pointed out in previous works [7,16], the WT can be seen as a mathematical microscope whose position and magnification are  $b$  and  $a^{-1}$ , respectively, and whose optics are given by the choice of the analyzing wavelet  $g$ . This microscope has proven to be well suited for studying local scaling properties of fractal objects [7,16,17]. Here, however, we will exploit its fascinating ability to reveal the structural hierarchy from which these scaling properties originate. As recently addressed in various theoretical studies [17,18], the wavelet analysis of singular measures does not require the analyzing wavelet  $g$  to be of zero mean. In the present study, we will use a Gaussian function  $g(x) = e^{-x^2/2}$ .

For a pedagogical purpose, we first show in Fig. 2(a) the WT representation in the  $(x,a)$  half plane of the uniform triadic Cantor set [16]. Indeed, we present only the skeleton defined by the positions of the local maxima [19,20] of  $|T_g(a,x)|$  considered as a function of  $x$ . (We refer the reader to Refs. [17] and [19] for a mathematical introduction to the WT modulus maxima representation.) Although we have reduced considerably the amount of data for the representation, the so-obtained treelike structure reveals the construction rule of the self-similar triadic Cantor set [16,17]. At the scale  $a = a_0 3^{-n}$ , each one of the  $k_0 2^n$  modulus maxima simultaneously bifurcates into two new maxima giving rise to a cascade of symmetric pitchfork branchings in the limit  $a \rightarrow 0$  ( $a_0$  and  $k_0$  are constants that depend on the specific shape of  $g$ ). The fractal dimension  $D_F = \ln 2 / \ln 3$  of the uniform triadic Cantor set can be directly obtained from the branching ratio  $r_B = 2$  and the scale factor (length ratio)  $r_L = 3$  be-

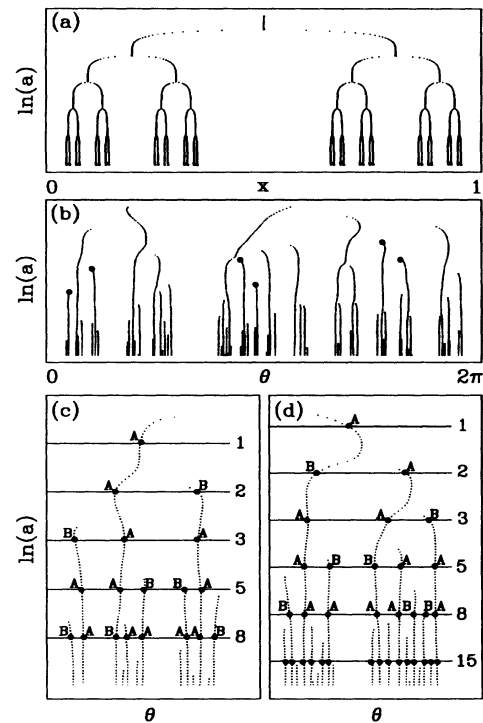


FIG. 2. WT skeleton defined from the local maxima of  $|T_g(a,x)|$  considered as a function of  $x$ . (a) The uniform triadic Cantor set. (b) The azimuthal Cantor set shown in Fig. 1(b). (c) and (d) are enlargements of the WT skeleton in (b) corresponding to two distinct main branches of the off-lattice DLA cluster in Fig. 1(a). The horizontal lines in (c) and (d) mark the scales  $a_n = a_0 r_L^{*-n}$  with  $r_L^* = 2.2$ ; the number of WT modulus maxima at each generation follows the Fibonacci series (4); moreover, a symbol  $A$  or  $B$  can be assigned to each of these maxima according to the Fibonacci recursive process (3). The analyzing wavelet  $g(x)$  is the Gaussian function.

tween two successive branchings, according to the general formula [17]

$$D_F = \ln r_B / \ln r_L. \quad (2)$$

The WT modulus maxima representation of the azimuthal Cantor set of a  $10^6$  particle DLA cluster is shown in Fig. 2(b). At first sight, one does not see any conspicuous recursive structure in the WT skeleton. One can, however, proceed to a systematic investigation of the value of the scale factor  $r_L$  between two successive bifurcations [black dots in Fig. 2(b)]. The result of the statistical analysis of 23 off-lattice clusters similar to the one shown in Fig. 1(a) is reported in Fig. 3. The distribution of scale factors displays a (unique) maximum at the value  $r_L^* = 2.2 \pm 0.2$ . Then, if one inserts the numerical values  $D_F^A = 0.60 \pm 0.02$  and  $r_L^* = 2.2 \pm 0.2$  into Eq. (2), one obtains a branching ratio  $r_B^* = (2.2)^{0.6} \sim 1.61$ . This numerical value is significantly different from 2, which unambiguously discards the possibility of an exact binary branching process. The most striking feature is that this

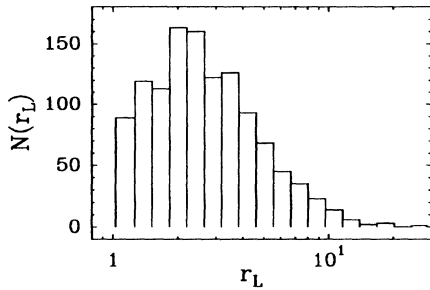


FIG. 3. Histogram of values of the scale factor  $r_L$  separating two successive bifurcations [● in Fig. 2(b)] in the WT modulus maxima skeleton of 23 DLA azimuthal Cantor sets. A single maximum is observed for  $r_L^* = 2.2 \pm 0.2$ .

value  $r_B^*$  is remarkably close to the golden mean  $\phi = (1 + \sqrt{5})/2 = 2 \cos(\pi/5) = 1.618\dots$

It is well known that the golden mean can be approached by means of successive Farey truncations  $W_n = F_{n+1}/F_n$  to its continued-fraction expansion, where  $F_n$  are Fibonacci numbers. Fibonacci sequences are naturally generated by the recursive process

$$A \rightarrow AB, \quad B \rightarrow A. \tag{3}$$

If one starts with the species  $B$  at generation  $n=0$ , one gets  $A$  at the generation  $n=1$ , and successively  $AB, ABA, ABAAB, ABAABABA, \dots$ . In other words, the population  $F_n$  at the generation  $n$  can be deduced from the two preceding populations,  $F_{n-1}$  and  $F_{n-2}$ , according to the iterative law

$$F_n = F_{n-1} + F_{n-2}, \quad F_0 = 1, \quad F_1 = 1. \tag{4}$$

(Notice that  $F_{n-1}$  and  $F_{n-2}$  are also the respective populations of  $A$  and  $B$  at step  $n$ .) In Figs. 2(c) and 2(d), we have magnified two regions of the WT skeleton in Fig. 2(b) corresponding respectively to two well-separated regions of the azimuthal Cantor set [Fig. 1(b)] issued from two distinct main branches of the considered off-lattice DLA cluster [Fig. 1(a)]. The horizontal lines in the  $(a, \theta)$  half plane are drawn as guide marks for the successive “generations” of WT modulus maxima. From the histogram in Fig. 3, these generations are (in a statistical sense) expected to occur at scales  $a_n = a_0 r_L^{*-n} = a_0 (2.2)^{-n}$ , where  $a_0$  is a constant that depends on the size of the DLA branch under study. The number of WT modulus maxima at each generation follows closely the Fibonacci series defined in Eq. (4). This observation corroborates our previous estimate of the branching ratio which is likely to behave like  $W_n = F_{n+1}/F_n$  and thus is expected to converge asymptotically to the golden mean. As indicated in Fig. 2(d), some deviations from the Fibonacci ordering are observed at small scales, but this is not so surprising since at scales  $a \sim$  a few particle sizes, the azimuthal Cantor set is very sensitive to small changes in the radius  $R$  of the circle which delimits the frozen region of the DLA clusters (Fig. 1). The overall

Fibonacci ordering is, however, rather robust with respect to the arbitrariness of the choice of this circle. As illustrated in Figs. 2(c) and 2(d), by assigning a symbol  $A$  or  $B$  at each maxima line issued from a bifurcation, one obtains a coding of the WT skeleton that complies with the recursive law (3). However, a systematic investigation of this coding for our statistical sample, reveals some randomness in the relative position of symbols  $A$  and  $B$  at the bifurcations  $A \rightarrow AB$ . Apparently  $B$  is equally likely to be found on the right or on the left of  $A$ . There exists also some arbitrariness in the spatial location of  $A$  when  $B$  proceeds to  $B \rightarrow A$ ; this arbitrariness is likely to result from local fluctuations in the value of the screening angle (about  $\theta^* = 36^\circ$ ) in the DLA branching morphology [9]. These fluctuations can produce some local departures from the Fibonacci ordering. A close examination of the WT skeleton in Fig. 2(b) reveals the presence of many of these defects. But the Fibonacci sequences are statistically predominant in the WT modulus maxima representations of the 23 off-lattice DLA azimuthal Cantor sets investigated in this study. A tentative interpretation of the numerical scale factor histogram in Fig. 3, in terms of Cantor set models which incorporate some randomness on top of a Fibonacci hierarchical structure, will be reported elsewhere.

A fundamental step in our demonstration is now to return to the DLA cluster itself and to point out Fibonacci sequences in its disordered branched morphology [9]. In Fig. 4, we use the two-dimensional WT microscope [7] to explore the internal structure of one main branch of a  $10^6$  particle off-lattice DLA cluster. The analyzing wavelet is the so-called Mexican hat. In Fig. 4(b), the magnification is chosen in order to reveal three successive branchings. These branchings proceed according to the Fibonacci recursion law (3) as identified by assigning a symbol  $A$  or  $B$  at the branches of successive generations. The original branch  $A$  gives two branches  $A$  and  $B$ ; both of these branches bifurcate into two new

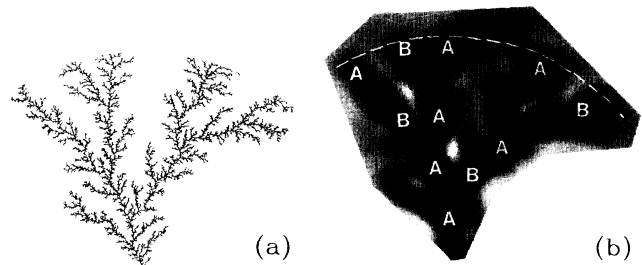


FIG. 4. One main extinct branch of a  $10^6$  particle off-lattice DLA cluster (a), as seen through the optics of the two-dimensional WT microscope (b). The analyzing wavelet is the Mexican hat  $g(\mathbf{x}) = (2 - |\mathbf{x}|^2)e^{-|\mathbf{x}|^2/2}$ .  $T_g$  is coded using 32 shades from white ( $T_g \leq 0$ ) to black ( $\max T_g > 0$ ). The magnification  $a^{-1}$  is such that three successive generations of branching are identified. At each branching, a symbol  $A$  or  $B$  can be assigned to the new branches according to the Fibonacci recursive process (3).

branches, but one of the branches issued from  $B$  is screened by the others and dies before reaching the reference circle that delimits the frozen region of the DLA aggregate. This peculiar electrostatic screening actually governs the growth process at each of its stages and originates in a statistical Fibonacci structural hierarchy [9]. Note that the observation of a perfect Fibonacci ordering coincides with a succession of screening angles [easily measurable in Fig. 4(b)] that do not significantly depart from  $\theta^* = 36^\circ$ . There may exist, however, important fluctuations in the screening angle value that can produce some local departure from the Fibonacci hierarchy. But despite the presence of these local structural defects, our statistical wavelet analysis of 23 off-lattice clusters attests that the DLA branching organization does exhibit a fascinating prevalent tendency to be Fibonacci. A systematic investigation of the actual relationship between the Fibonacci branching ordering and the structural fivefold symmetry is currently in progress.

To summarize, we have reported the discovery of Fibonacci sequences in the frozen morphology of large mass off-lattice DLA clusters. This observation is consistent with a preferential branching ratio that converges asymptotically to the golden mean. This statistical hidden hierarchy is likely to be intimately related to the structural fivefold symmetry that underlies the self-similarity of DLA clusters. These results provide an important clue to the theoretical understanding of diffusion-limited aggregation and should guide future work addressing the crucial issue of the selection mechanism of the DLA morphology.

We would like to thank Y. Couder and V. Hakim for interesting discussions and J. Huth for a careful reading of the manuscript. This work was supported by the Direction des Recherches Etudes et Techniques under Contract DRET No. 89/196 and the Centre National des Etudes Spatiales under Contract No. 91/CNES/0323.

<sup>(a)</sup>Present address: Ecole Normale Supérieure, 45 rue d'Ulm, 75005 Paris, France.

- [1] *The Physics of Structure Formation*, edited by W. Guttinger and D. Dangelmayr (Springer, Berlin, 1987); *Random Fluctuations and Pattern Growth*, edited by H. E. Stanley and N. Ostrowsky (Kluwer, Dordrecht, 1988); J. Feder, *Fractals* (Pergamon, New York, 1988); T. Vicsek, *Fractal Growth Phenomena* (World Scientific, Singapore, 1989).
- [2] T. Witten and L. M. Sander, *Phys. Rev. Lett.* **47**, 1400 (1981); *Phys. Rev. B* **27**, 5868 (1983).
- [3] P. Meakin, in *Phase Transitions and Critical Phenomena*, edited by C. Domb and J. L. Lebowitz (Academic, Orlando, 1988), Vol. 12.
- [4] R. C. Ball, R. M. Brady, G. Rossi, and B. R. Thompson, *Phys. Rev. Lett.* **55**, 1406 (1985); M. Kolb, *J. Phys. (Paris), Lett.* **46**, L631 (1985); P. Meakin and T. Vicsek, *Phys. Rev. A* **32**, 685 (1985); P. Meakin, *Phys. Rev. A* **33**, 3371 (1986); P. Meakin, R. C. Ball, P. Ramanlal, and L. M. Sander, *Phys. Rev. A* **35**, 5233 (1987).
- [5] (a) G. Li, L. M. Sander, and P. Meakin, *Phys. Rev. Lett.* **63**, 1322 (1989); (b) P. Ossadnik, *Phys. Rev. A* **45**, 1058 (1992).
- [6] F. Argoul, A. Arneodo, G. Grasseau, and H. L. Swinney, *Phys. Rev. Lett.* **61**, 2558 (1988); **63**, 1323 (1989).
- [7] F. Argoul, A. Arneodo, J. Elezgaray, G. Grasseau, and R. Murenzi, *Phys. Lett. A* **135**, 327 (1989); *Phys. Rev. A* **41**, 5537 (1990).
- [8] Box-counting and fixed-mass algorithms [6,7] and, more recently, the investigation of the scaling exponents of both the length and the width of the branches of large mass ( $M = 10^7$ ) off-lattice DLA clusters [5(b)] have confirmed the estimate  $D_F = 1.60 \pm 0.02$ . This value is significantly smaller than the dynamical dimension  $D_d = 1.71 \pm 0.02$  deduced from the evolution of the radius of gyration versus the mass during cluster growth [2,3]. Both of these dimensions do not seem to converge asymptotically to a unique value, as commonly believed.
- [9] A. Arneodo, F. Argoul, J. F. Muzy, and M. Tabard, "Uncovering Fibonacci Sequences in the Fractal Morphology of Diffusion-Limited Aggregates" (to be published).
- [10] R. C. Ball, *Physica (Amsterdam)* **140A**, 62 (1986); T. C. Halsey, P. Meakin, and I. Procaccia, *Phys. Rev. Lett.* **56**, 854 (1986); I. Procaccia and R. Zeitak, *Phys. Rev. Lett.* **60**, 2511 (1988).
- [11] B. Derrida, V. Hakim, and J. Vannimenus, *Phys. Rev. A* **43**, 888 (1991).
- [12] R. C. Ball and R. M. Brady, *J. Phys. A* **18**, L809 (1985).
- [13] M. Plischke and Z. Rácz, *Phys. Rev. Lett.* **53**, 415 (1984).
- [14] F. Argoul, A. Arneodo, J. Elezgaray, and G. Grasseau, in *Measure of Complexity and Chaos*, edited by N. B. Abraham, A. M. Albano, A. Passamante, and P. E. Rapp (Plenum, New York, 1989), p. 433; C. Amitrano, P. Meakin, and H. E. Stanley, *Phys. Rev. A* **40**, 1713 (1989).
- [15] B. B. Mandelbrot, *J. Stat. Phys.* **34**, 895 (1984); in *Fractals' Physical Origin and Properties*, edited by L. Pietronero (Plenum, New York, 1989).
- [16] A. Arneodo, G. Grasseau, and M. Holschneider, *Phys. Rev. Lett.* **61**, 2281 (1988); in *Wavelets*, edited by J. M. Combes, A. Grossmann, and P. Tchamitchian (Springer, Berlin, 1989), p. 182; A. Arneodo, F. Argoul, J. Elezgaray, and G. Grasseau, in *Nonlinear Dynamics*, edited by G. Turchetti (World Scientific, Singapore, 1988), p. 130.
- [17] J. F. Muzy, E. Bacry, and A. Arneodo, *Phys. Rev. Lett.* **67**, 3515 (1991); A. Arneodo, E. Bacry, and J. F. Muzy, "Wavelet Analysis of Fractal Signals: Direct Determination of the Singularity Spectrum of Fully Developed Turbulence Data (Springer, Berlin, to be published); E. Bacry, J. F. Muzy, and A. Arneodo, "Singularity Spectrum of Fractal Signals from Wavelet Analysis: Exact Results" (to be published).
- [18] J. M. Ghez and S. Vaienti, "Integrated Wavelets on Fractal Sets. II The generalized Fractal Dimensions" (to be published).
- [19] A. Mallat and S. Zhong, New York University Technical Report No. 483 (Computer Science Department, 1989).
- [20] Note that a complete description of the scaling properties of multifractal measures requires both the locations and the values of the WT modula maxima (see Ref. [17]).

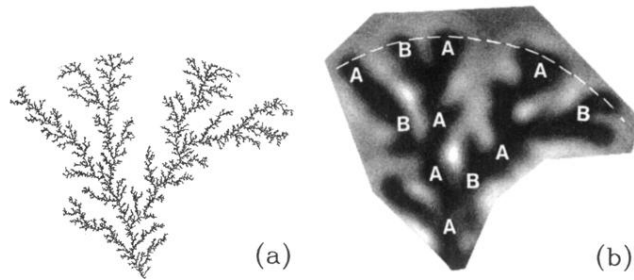


FIG. 4. One main extinct branch of a  $10^6$  particle off-lattice DLA cluster (a), as seen through the optics of the two-dimensional WT microscope (b). The analyzing wavelet is the Mexican hat  $g(\mathbf{x}) = (2 - |\mathbf{x}|^2)e^{-|\mathbf{x}|^2/2}$ .  $T_g$  is coded using 32 shades from white ( $T_g \leq 0$ ) to black ( $\max T_g > 0$ ). The magnification  $a^{-1}$  is such that three successive generations of branching are identified. At each branching, a symbol  $A$  or  $B$  can be assigned to the new branches according to the Fibonacci recursive process (3).